Molecular Scaffolding of Prussian Blue Analogues Using a Phenanthroline-Extended Triptycene Ligand

4 AUTHORS, INCLUDING:

Xavier Roy
Columbia University

23 PUBLICATIONS   **354** CITATIONS

SEE PROFILE

Mark J MacLachlan
University of British Columbia - Vancouver

167 PUBLICATIONS   **5,282** CITATIONS

SEE PROFILE

Molecular Scaffolding of Prussian Blue Analogues Using a Phenanthroline-Extended Triptycene Ligand

Xavier Roy, Jonathan H. Chong, Brian O. Patrick, and Mark J. MacLachlan*

Department of Chemistry, University of British Columbia, 2036 Main Mall, Vancouver, British Columbia, Canada V6T 1Z1

S *Supporting Information*

ABSTRACT: Shape-persistent ligands with triptycene groups are promising candidates for the development of porous metal—organic frameworks with functional surface area. In this work, a series of phenanthroline-extended triptycene compounds was synthesized and used as structure-directing ligands for the fabrication of a triptycene-scaffolded Prussian blue analogue. The ligands were reacted with $K_3[Fe(CN)_6]$ and $CuCl_2$ under hydrothermal conditions to afford two new clathrates: a coordination compound of (triptycenyl phenanthroline) copper(I) and an infinite one-dimensional zigzag coordination polymer of copper cyanide scaffolded by phenanthroline-extended triptycenes. These structures illustrate the potential for the triptycene-functionalized ligands to provide access to materials with interesting architectures.
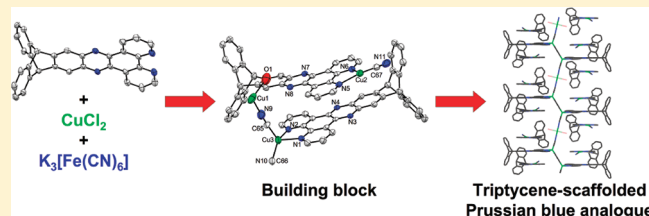
INTRODUCTION

Coordination polymers (CPs) have metal ions linked together into an infinite network by bridging ligands. Although the first synthetic CP, Prussian blue (PB), was discovered as early as 1704, these materials received little attention until landmark reports by Robson and Hoskins that introduced the concept of a net-based approach for the design of CPs.[1,2] The idea of 'engineering' the structure of CPs through rational design in order to achieve desired properties revolutionized the field and led to the discovery of some of the most exciting functional materials of the past 15 years.[3−7]

Prussian blue (PB) is the archetype CP. It is a three-dimensional cubic network of $Fe_4[Fe(CN)_6]_3 \cdot nH_2O$ in which the Fe atoms (Fe^{II} and Fe^{III}) lie at the lattice points and the cyanide groups are bridging. The PB framework is thermodynamically stable and obtained for a wide range of Prussian blue analogues (PBAs). Recently, cyanide ligands have been employed in a large number of CPs to create materials with diverse properties.[8−11] Cyanide ligands are interesting because they promote strong spin coupling between the bridged metal ions through superexchange interactions, and PBAs have been extensively investigated for their magnetic properties.[12] On the other hand, the internal surface area of these materials is usually inaccessible to guest molecules because the pores made by bridging cyanides are too small and not interconnected. Recently, a certain degree of control over the structure of the network was achieved by changing the oxidation state of the metal ions in the PBA[13] and using metals with different coordination geometries.[14,15] PBAs with bigger pores made from cyanide-capped metal clusters[16] and incorporating a third building block have also been reported.[17]

Another approach to engineering the network of PBAs is to incorporate structure-directing ligands into the assembly. To achieve this, one can use PBA precursors that are precoordinated with ligands such as 2,2′-bipyridine[18,19] or nitrosyl[20] or incorporate the organic structure-directing compounds into the PBA network under hydrothermal conditions.[21−27] In the latter approach, the cyanide ligands become labile at high temperature and the thermodynamic product is obtained. In addition to introducing new functional units into the materials, one can control the dimensionality of the PBA network using this technique. For instance, fabrication of mixed-ligand heterometallic Cu^I/Fe^{II} and homometallic Cu^I PBAs under hydrothermal conditions has been extensively studied, and one-dimensional chains,[24,25] two-dimensional layers,[22] and three-dimensional frameworks[21] have been synthesized using 1,10-phenanthroline and 2,2′-bipyridine as chelating ligands. Other structure-modified bimetallic PBAs containing Ni/Co and Cr/Mn have also been reported.[18,23]

Triptycene is a rigid polyaromatic molecule best known for its three-dimensional paddlewheel shape. It is an attractive building block for the fabrication of solid-state nanostructures because it has a large internal molecular free volume (IMFV) conferred by its rigid three-dimensional paddlewheel geometry that resists effective packing. Triptycene has been investigated as a porosity-generating compound in a number of materials, and a few derivatives have been used in the fabrication of CPs and MOFs.[28−36] However, to the best of our knowledge, triptycene has never been incorporated into PBAs.

Recently, Jiang et al. reported a new family of phenanthroline-extended triptycenes that could potentially be used as rigid scaffolding ligands for the fabrication of novel CPs and molecular solid-state assemblies.[37] Unfortunately, no coordination complexes
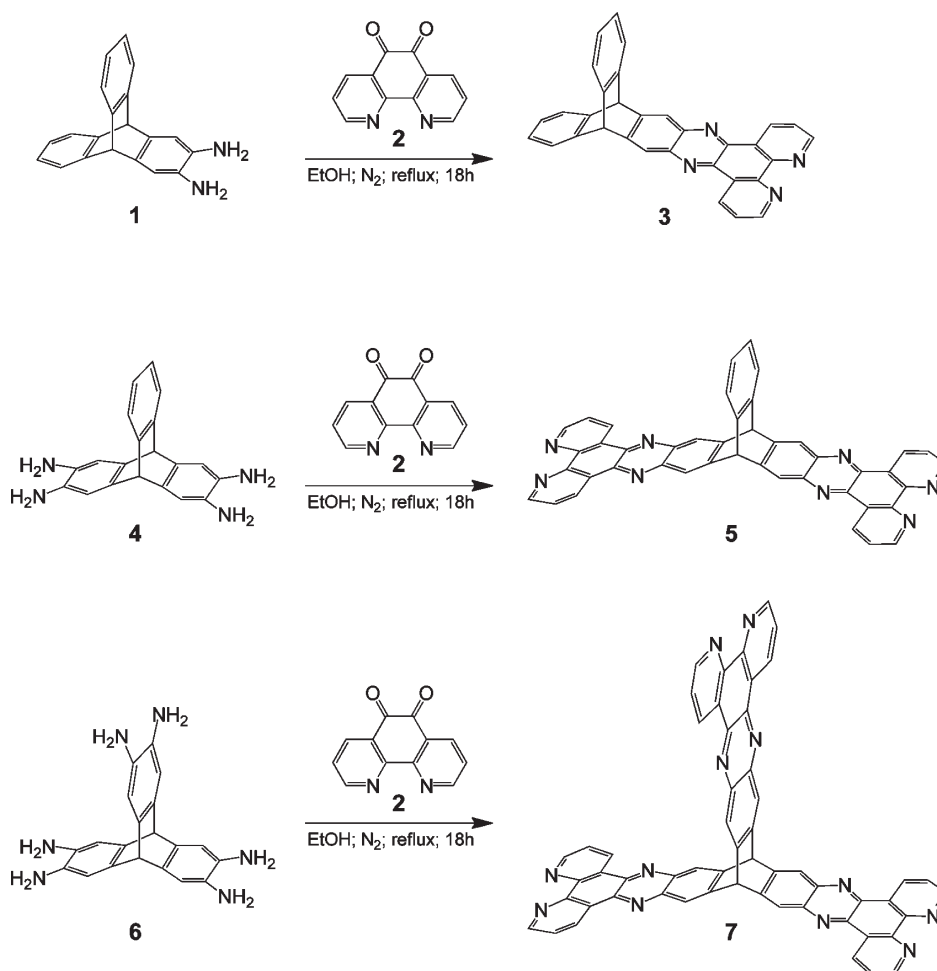
Figure 1. Synthesis of phenanthroline-extended triptycenes **3**, **5**, and **7**.

incorporating these chelating ligands were reported. In this article, we expand the range of accessible phenanthroline-extended triptycenes and describe a synthetic strategy to prepare solid-state CPs based on these compounds. We selected the inorganic compounds $CuCl_2$ and $K_3[Fe(CN)_6]$ as starting materials for the preparation of triptycene-scaffolded PBAs because they are known to form PBAs that incorporate a variety of chelating ligands under hydrothermal conditions. A novel triptycene-coordinated Cu^I molecular complex is also discussed en route to the triptycene-scaffolded PBA.

■ EXPERIMENTAL SECTION

Starting Materials and General Methods. The polyamino-triptycenes **1**, **4**, and **6** were prepared according to published procedures (see Figure 1 for the structures).[30] 1,10-Phenanthroline-5,6-dione (**2**) was prepared according to the procedure by Amouyal et al.[38] The reactions to prepare the phenanthroline-extended triptycene compounds were performed under a nitrogen atmosphere, and the solvents were sparged with nitrogen before use.

The solvothermal reactions were performed in 22 mL Parr pressure vessels equipped with Teflon liners. A maximum of 10 mL of solvent was used for the solvothermal reactions. The pressure vessels were placed in a preheated programmable oven for the indicated time and then cooled to room temperature at a rate of 7 °C h^{-1}.

Triptycenyl Phenanthroline (3). A solution of 2,3-diaminotrip-tycene (**1**) (200 mg, 0.70 mmol) and **2** (171 mg, 0.81 mmol) in ethanol (40 mL) was heated to reflux under a nitrogen atmosphere for 18 h. After cooling to room temperature, the precipitate was collected by suction filtration and washed with ethanol. Vacuum drying at 50 °C yielded the desired product as a pale yellow solid (260 mg, 81% yield). Single crystals of **3** were obtained by heating a suspension of **3** (5 mg, 11 μmol) in 10 mL of methanol in a pressure vessel at 180 °C for 24 h and then slowly cooling the pressure vessel.

*Data for **3**.* ^{1}H NMR (400 MHz, CDCl$_3$): δ 9.57 (d of d, ^3J(H,H) = 2,8 Hz, 2H, CH), 9.22 (d of d, ^3J(H,H) = 2,4 Hz, 2H, CH), 8.24 (s, 2H, CH), 7.74 (d of d, ^3J(H,H) = 4,8 Hz, 2H, CH), 7.54−7.52 (m, 4H, CH), 7.13−7.10 (m, 4H, CH), 5.74 (s, 2H, bridgehead). ^{13}C NMR (100.6 MHz, CDCl$_3$): δ 152.1, 147.9, 147.0, 143.5, 141.6, 140.2, 133.3, 127.4, 126.2, 124.1, 123.8, 122.7, 53.7. HR-MS (EI, 70 eV) calcd for C$_{32}$H$_{18}$N$_4$: 458.15315. Found: 458.15394. IR $\bar{\nu}$ = 3350, 2967, 1574, 1479, 1448, 1430, 1401, 1358, 1336, 1315, 1273, 1150, 1122, 1109, 1071, 1053, 1029, 893, 807, 767, 749, 736, 628, 597, 564, 492, 481 cm^{-1}. Mp > 300 °C.

Triptycenyl Bis(phenanthroline) (5). A solution of 2,3,6,7-tetraaminotriptycene (**4**) (95 mg, 0.30 mmol) and **2** (142 mg, 0.68 mmol) in ethanol (40 mL) was heated to reflux under a nitrogen atmosphere for 18 h. After cooling to room temperature, the precipitate was collected by suction filtration and washed with ethanol. Vacuum drying at 50 °C yielded the desired product as a light brown, shiny solid (186 mg, 93% yield).

*Data for **5**.* ^{1}H NMR (400 MHz, CD$_2$Cl$_2$): δ 9.61 (d of d, ^3J(H,H) = 2,8 Hz, 4H, CH), 9.18 (d of d, ^3J(H,H) = 2,5 Hz, 4H, CH), 8.44 (s, 4H,

Table 1. Selected Crystallographic Data for Compounds 3, 8, and 9

compound	3	8	9
formula	$C_{32.5}H_{20}N_4O_{0.5}$	$C_{128}H_{72}N_{16}Cl_4Cu_4O$	$C_{69.5}H_{49}N_{10.5}Cu_{2.5}O_{3.5}$
MW	474.53	2245.98	1246.04
lattice type	monoclinic	monoclinic	monoclinic
space group	$P2_1/n$	$C2/c$	$P2_1/c$
a (Å)	8.011(2)	88.779(12)	15.577(2)
b (Å)	30.610(3)	8.2340(11)	27.390(3)
c (Å)	18.451(8)	27.418(4)	13.570(1)
α (deg)	90	90	90
β (deg)	97.264(4)	102.6170(10)	96.227(3)
γ (deg)	90	90	90
V (Å^3)	4488.4(7)	19559(5)	5755.3(9)
Z value	8	8	4
D_{calcd} (g cm^{-3})	1.404	1.525	1.385
T (K)	173	150	90
GOF on F^2	0.974	0.994	1.13
$R_1{}^a [I > 2\sigma(I)]$	0.0531	0.0526	0.073
$wR_2{}^b$ (all data)	0.1182	0.1390	0.194

$^a R_1 = (\Sigma||F_o| - |F_c||)/(\Sigma|F_o|).$ $^b wR_2 = [(\Sigma w(F_o{}^2 - F_c{}^2)^2)/(\Sigma w(F_o{}^2)^2)]^{1/2}.$

CH), 7.77 (d of d, ^3J(H,H) = 4,8 Hz, 4H, CH), 7.71−7.68 (m, 2H, CH), 7.24−7.22 (m, 2H, CH), 6.13 (s, 2H, bridgehead). ^{13}C NMR (100.6 MHz, CDCl$_3$): δ 152.4, 145.4, 142.1, 141.8, 140.8, 133.6, 127.5, 127.1, 125.6, 124.6, 124.1, 123.7, 53.5. HR-MS (EI, 70 eV) calcd for C$_{44}$H$_{22}$N$_8$: 662.19674. Found: 662.19507. IR $\bar{\nu}$ = 3360, 1633, 1574, 1478, 1448, 1418, 1402, 1358, 1337, 1228, 1197, 1165, 1149, 1128, 1107, 1070, 1030, 890, 808, 760, 738, 629, 608, 593, 564, 490 cm^{-1}. Mp > 300 °C.

Triptycenyl Tris(phenanthroline) (7). A solution of 2,3,6,7,14,15-hexaaminotriptycene (**7**) (100 mg, 0.29 mmol) and **2** (197 mg, 0.94 mmol) in ethanol (30 mL) was heated to reflux under a nitrogen atmosphere for 18 h. After cooling to room temperature, the precipitate was collected by suction filtration and washed with ethanol. Vacuum drying at 50 °C yielded the desired product as a brown solid (137 mg, 54% yield).

Data for **7.** ^{1}H NMR (400 MHz, CDCl$_3$): δ 9.65 (d of d, ^3J(H,H) = 2,8 Hz, 6H, CH), 9.29 (d of d, ^3J(H,H) = 2,4 Hz, 6H, CH), 8.60 (s, 6H, CH), 7.82 (d of d, ^3J(H,H) = 4,8 Hz, 6H, CH), 6.43 (s, 2H, bridgehead). HR-MS (ESI, MeOH) calcd for C$_{56}$H$_{27}$N$_{12}$: 867.2482 ([M + H]$^+$). Found: 867.2499. IR $\bar{\nu}$ = 3390, 1633, 1537, 1478, 1447, 1402, 1357, 1338, 1228, 1198, 1123, 1070, 1030, 889, 807, 740, 616, 597, 564, 491 cm^{-1}. Mp > 300 °C. Insufficient solubility for ^{13}C NMR spectroscopy.

Triptycene-Scaffolded PBA (9). Triptycenyl phenanthroline (**3**, 10.0 mg, 22 μmol), CuCl$_2$·2H$_2$O (3.7 mg, 22 μmol), K$_3$[Fe(CN)$_6$] (7.2 mg, 22 μmol), and 10 mL of methanol were loaded into a Parr pressure vessel equipped with a Teflon liner. The pressure vessel was placed in a preheated programmable oven at 180 °C for 48 h. The reaction was then cooled to room temperature using a controlled ramp of 7 °C h^{-1}. A mixture of black needles (**8**), orange plates (**9**), and brown cubes (**10**) was obtained. The black needles and brown cubes were decanted off, while the orange plates stuck to the walls of the Teflon liner. The black needles aggregated into a wool-type material that was easily separated from the brown cubes using tweezers. The orange plates were suspended in methanol by sonication. All of the materials were kept in methanol until X-ray diffraction crystallographic characterization. Compound **9** was isolated by centrifugation at 4500 rpm, washed with dichloromethane, and dried under vacuum for at 60 °C for 24 h. Yield: 4.0 mg of orange plates (37% based on Cu).

X-ray diffraction analysis of **9** suggests a chemical formula of C$_{66.5}$H$_{36}$N$_{10.5}$Cu$_{2.5}$·[0.5H$_2$O] along with three methanol guest molecules in the asymmetric unit. The sample submitted for elemental analysis (EA) was dried under vacuum at 60 °C for 24 h to remove as much guest solvent as possible. The dried structures most likely adsorbed water upon standing in air. Satisfactory EA of **9** was obtained assuming 1.5 H$_2$O and 1 CH$_3$OH guest molecules per asymmetric unit in the structure. Anal. Calcd for C$_{66.5}$H$_{36}$N$_{10.5}$Cu$_{2.5}$·[0.5H$_2$O]·1.5H$_2$O·CH$_3$OH: C, 67.06; H, 3.67; N, 12.16. Found: C, 66.94; H, 3.36; N, 12.25.

Alternate Synthesis of (Triptycenyl phenanthroline)-copper(I) Complex (8*). X-ray diffraction analysis of **8** suggests a chemical formula of C$_{128}$H$_{72}$N$_{16}$Cl$_4$Cu$_4$O: a single peak of electronic density corresponding to one oxygen atom was detected in the asymmetric unit. This oxygen is probably from a guest water molecule.

As **8** was always found combined with **9** and **10**, we attempted its direct synthesis after determining its single-crystal X-ray structure. Triptycenyl phenanthroline (**3**, 17.1 mg, 37 μmol), CuCl$_2$·2H$_2$O (6.3 mg, 37 μmol), and 10 mL of methanol were loaded into a Parr pressure vessel equipped with a Teflon liner. The pressure vessel was placed in a preheated programmable oven at 180 °C for 24 h. The reaction mixture was then cooled to room temperature using a controlled ramp of 7 °C h^{-1}. Black needles (**8***) were obtained as the only product, and they looked identical to **8**. The needles were centrifuged at 4500 rpm, washed with dichloromethane, and dried under vacuum at 60 °C for 24 h. Yield: 18.1 mg of crystalline black solid (88% based on Cu). The sample submitted for EA was dried under vacuum at 60 °C for 24 h to remove as much guest solvent as possible. Satisfactory EA of **8*** was obtained assuming that no guest molecules are present in the structure. Anal. Calcd for C$_{128}$H$_{72}$N$_{16}$Cl$_4$Cu$_4$: C, 68.94; H, 3.25; N, 10.05. Found: C, 68.71; H, 3.38; N, 10.26.

Single-Crystal X-ray Diffraction (SCXRD) Analysis. Crystals of compounds **3**, **8**, and **9** were mounted on a glass fiber with oil. Diffraction data for **3** were collected on a Bruker X8 diffractometer using graphite-monochromated Mo Kα radiation. Intensity data for **8** were collected on a D8 goniostat equipped with a Bruker APEX II CCD detector at Beamline 11.3.1 at the Advanced Light Source (Lawrence Berkeley National Laboratory) using synchrotron radiation tuned to λ = 0.7749 Å. Measurements for compound **9** were made on a Bruker APEX DUO diffractometer with graphite-monochromated Cu Kα radiation. Structure solutions were refined using the SHELXL software. Specific details regarding refinement are provided in the Supporting Information. Table 1 summarizes the main crystallographic parameters.

■ RESULTS AND DISCUSSION

The phenanthroline-extended triptycenes **3**, **5**, and **7** were prepared by Schiff-base condensation of 1,10-phenanthroline-5,6-dione (**2**) with the polyaminotriptycenes **1**, **4**, and **6**, respectively (Figure 1). Compound **3** is known, but only the *n*-butyl and *tert*-butyl derivatives of **7** have previously been reported because of solubility issues. Satisfactory ^{1}H NMR and electrospray ionization mass spectra of **7** were nonetheless obtained in this work, although ^{13}C NMR spectroscopy could not be performed because of the low solubility of **7**. Compound **5**, which has never been reported, was fully characterized. In the ^{1}H NMR spectrum, the most diagnostic resonance is the one assigned to the bridgehead CH group, which moves consistently downfield with addition of dipyrido[3,2-a:2',3'-c]phenazine (dppz) groups (from 5.40 ppm for triptycene to 6.43 ppm in **7**).

Single crystals of **3** were obtained by heating a suspension of the compound in methanol to 180 °C in a Parr pressure vessel for 48 h. Compound **3** is presumably partially soluble in methanol at that temperature, and single crystals were grown by slowly cooling the pressure vessel. Figure 2a shows the solid-state
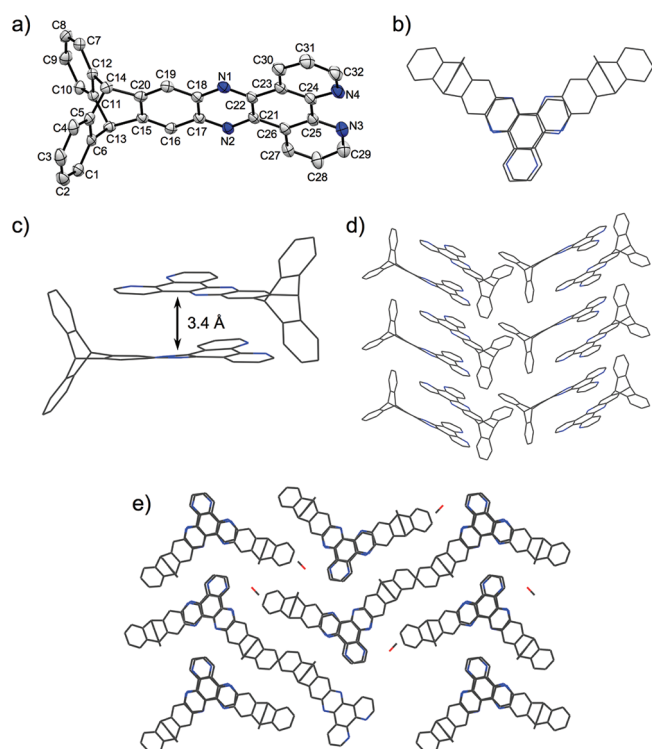
Figure 2. Molecular structure of **3** ($C_{32.5}H_{20}N_4O_{0.5}$) in the solid state as determined by SCXRD. Hydrogen atoms have been omitted for clarity: carbon, gray; nitrogen, blue; oxygen, red. (a) ORTEP of a single molecule. Ellipsoids are shown at the 50% probability level. (b) View showing stacking of a pair of molecules. (c) Side view of a pair of stacked molecules. (d) View down the *c* axis showing stacks extending along the *a* axis. (Guest solvent molecules have been omitted for clarity in a–d.) (e) View down the *a* axis showing solvent-filled channels (the methanol molecules are shown in this case).

structure for **3**. The extended packing arrangement along the *a* axis shows partial overlap of the aromatic rings in the phenanthroline moiety, with the rings separated by approximately 3.4 Å, which is an optimal distance for π stacking (Figure 2b, 2c, and 2d). While stacking typically improves packing efficiency, the rigid bulky triptycene moieties force the molecules to adopt a staggered conformation within the stacks (staggering angle is ca. 120°) and prevent the stacks from assembling into a close-packed structure. The stacks instead adopt an *up–down* or undulating arrangement along the *b* axis (Figure 2e). The unfilled space between the stacks contains guest methanol molecules, producing solvent-filled channels that extend along the direction of the *a* axis (Figure 2e).

We attempted to synthesize triptycene-scaffolded PBAs from compounds **3**, **5**, and **7** under solvothermal conditions. It was anticipated that the combination of high temperature and high pressure would help dissolve the starting materials, provide enough thermal energy to labilize the cyanide ligands, and assist in the incorporation of the phenanthroline-extended triptycene ligands into the PBA framework. In addition, slow cooling of the reaction mixture should facilitate growth of single crystals suitable for X-ray diffraction characterization.

Triptycenyl phenanthroline **3**, $CuCl_2$, and $K_3[Fe(CN)_6]$ were combined with methanol in a Parr pressure vessel and heated to 180 °C for 48 h. A mixture of crystalline products was obtained upon cooling the reaction: thin black needles (**8**), orange plates

(**9**), and brown cubes (**10**). Because of the extremely small size of the black needles, X-ray diffraction of **8** was performed using synchrotron radiation. The solid-state structure of **8** shows two ligands **3** chelating one copper atom; the pseudotetrahedral geometry at the metal center suggests that it is in the +1 oxidation state (Figure 3a). The charge balance of the structure is also consistent with a Cu^I species: the +1 charge on the chelated metal is balanced by one $[CuCl_2]^-$ counterion in its vicinity. Under the reaction conditions (high temperature and high pressure), the Cu^{II} ions are most likely reduced to Cu^I by methanol, the *N*-heterocyclic compounds, or free cyanides from dissociation of $[Fe(CN)_6]^{3-}$ (or a combination of these species) acting as the reducing agent.[21,22] Although somewhat unusual, the anion $[CuCl_2]^-$ has nonetheless been observed and characterized crystallographically several times.[39] Figures 3b and 3c show the extended structure of **8**. The copper atoms assemble into columns along the *b* axis, with some interdigitation of the triptycenes along the *c* axis. Two types of stacking arrangement are observed for ligand **3**: one with no significant overlap along the stacks, and one with some amount of overlap between the phenanthrolines, although there is a slight deviation from coplanarity (Figure 3b). The distance between the ligand dppz moieties in the overlapping stacks is approximately 3.2 Å, which suggests π stacking. The presence of the triptycenes and the constraints imposed by the tetrahedral metal center hinder packing, resulting in void channels running along the direction of the *b* axis (Figure 3b). The voids are partially filled by the $[CuCl_2]^-$ counterions, and a single peak of electronic density that was satisfactorily modeled as an oxygen atom was also detected in the asymmetric unit (not shown in Figure 3). This oxygen is probably from a guest water molecule since there is no residual electronic density to suggest that it is a methanol molecule.

In order to investigate the formation of compound **8** with the goal of achieving a selective synthesis of this complex, the same solvothermal reaction was performed for two different periods of 12 h and 5 days. The mixture of products obtained after 5 days is similar to the one obtained after 48 h of reaction, but the product obtained after only 12 h contained almost exclusively black needles. Resuming the solvothermal reaction at 180 °C in methanol for an additional 36 h and reusing the 12 h synthesis product as starting material yielded the usual mixture of orange plates (**9**) and brown cubes (**10**) along with a small fraction of black needles (**8**). These results suggest that the copper ions (reduced to Cu^I or not) first react with **3** to form complex **8**, and this compound is then slowly converted to **9** and **10** upon further heating.

The direct solvothermal synthesis of **8** (without addition of $K_3[Fe(CN)_6]$) was also attempted by reacting 1 equiv of **3** with 1 equiv of $CuCl_2$ in methanol at 180 °C for 24 h. Black crystalline needles (**8***) akin to **8** were obtained in high yield. Powder X-ray diffraction (PXRD) experiments were performed on **8***, and the experimental data was compared with the PXRD pattern of **8** calculated from the single-crystal data (Figure 4). Although not identical, the two patterns are in good agreement, supporting the direct preparation of **8**. The variations between the patterns may be explained by the different amounts of solvent molecules trapped in the structures and a partial collapse of the structure upon drying of solid **8***. Elemental analysis (EA) provides further evidence for direct solvothermal synthesis of **8**. Compound **8*** has the same C, H, and N composition as **8** ($[(\mathbf{3})_2Cu]^+[CuCl_2]^-$). Finally, the IR spectrum of **8*** shows a number of peaks that belong to **3**. No peaks that can be assigned
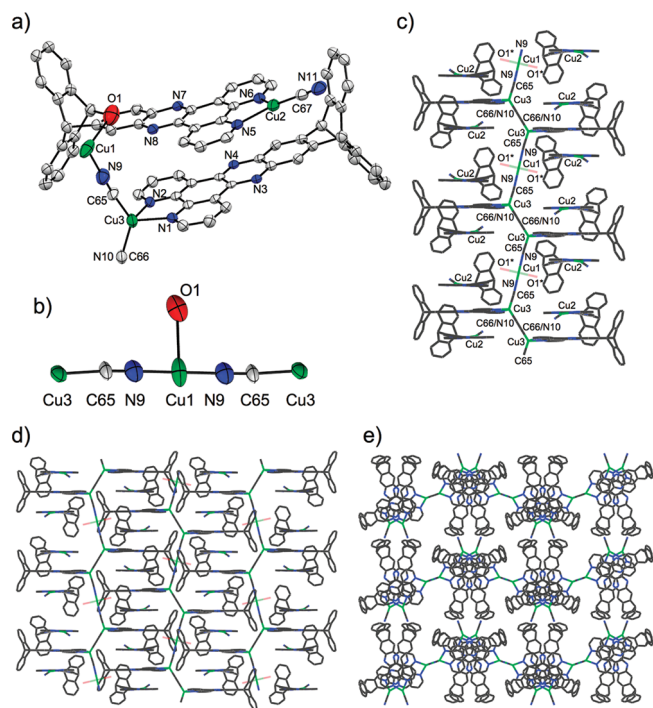
a)

b)

c)
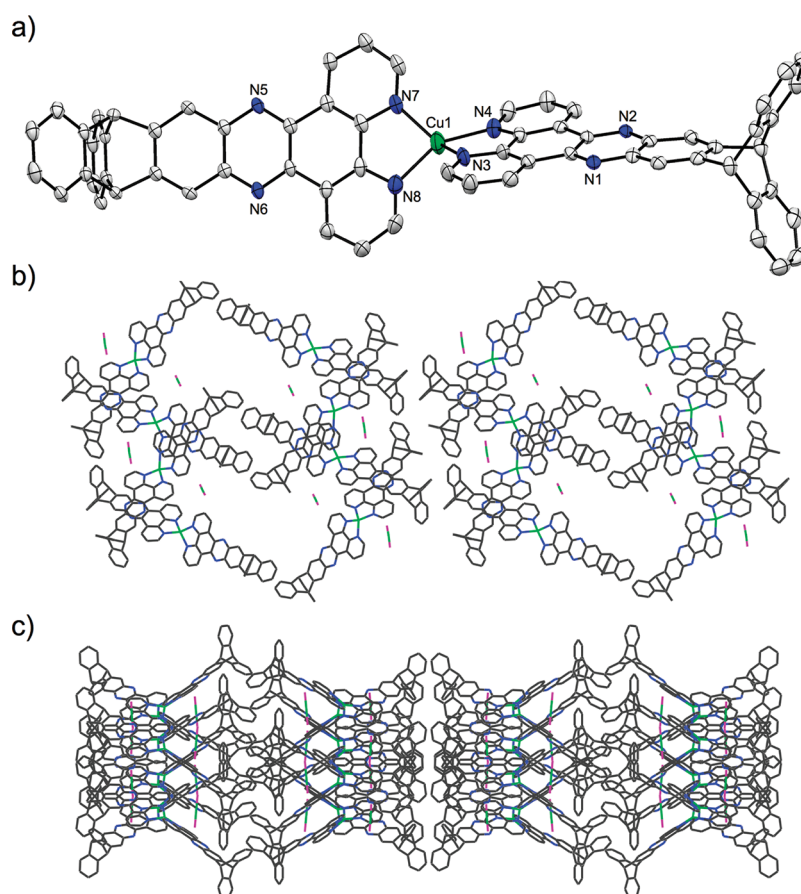
Figure 3. Molecular structure of **8** ($C_{128}H_{72}N_{16}Cl_4Cu_4O$) in the solid state as determined by SCXRD. Hydrogen atoms and solvent molecules have been omitted for clarity: carbon, gray; nitrogen, blue; copper, green; chlorine, pink. (a) ORTEP of a single metal complex. The $[CuCl_2]^-$ couterion and carbon atom labels on the triptycene ligands have been omitted for clarity. Ellipsoids are shown at the 50% probability level. (b) View down the *b* axis showing the void channels and the interdigitation of the triptycenes. (c) View down the *c* axis showing the Cu^I atom columns. $[CuCl_2]^-$ counterions are included in b and c.
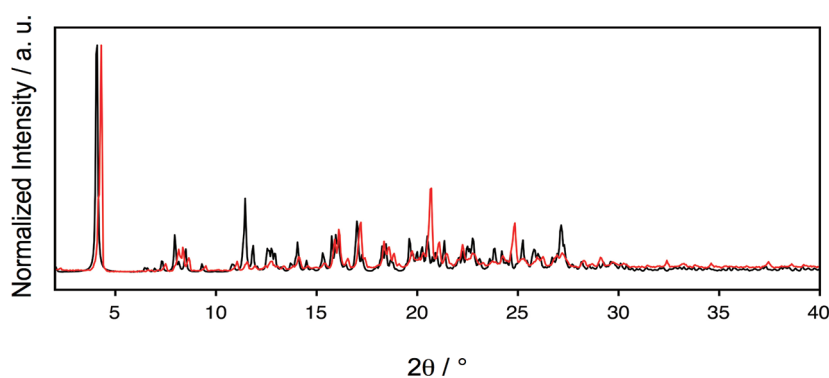
Figure 4. PXRD patterns of the black needles synthesized using two different approaches. The black trace is the calculated PXRD pattern of **8** (calculated from the single-crystal data). The red trace is the experimental PXRD pattern of **8*** (as prepared without $K_3[Fe(CN)_6]$). The variations between the patterns may be explained by the different amounts of solvent molecules trapped in the structures and a partial collapse of the structure upon drying of the powder prior to PXRD analysis.

to cyanide ligands are observed. All of these results suggest that **8** can be synthesized directly without addition of $K_3[Fe(CN)_6]$. In this case, methanol or the *N*-heterocyclic compounds most likely act as the reducing agent. Interestingly, reacting **3** with CuCl under the same conditions did not yield the expected crystalline product.

The solid-state crystal structure of **8** suggests a porous structure that may have a sizable surface area. Nitrogen adsorption experiments were performed to further investigate this question, but unfortunately, no surface area could be measured for these materials. The porous structure probably collapses upon removal of the guest solvent molecules under vacuum. These results are

Figure 5. Molecular structure of **9** ($C_{69.5}H_{49}N_{10.5}Cu_{2.5}O_{3.5}$) in the solid state as determined by SCXRD. Hydrogen atoms, guest solvent molecules, and carbon atom labels on the triptycene ligands have been omitted for clarity: carbon, gray; nitrogen, blue; oxygen, red; copper, green. (a) ORTEP for the repeating unit of the triptycene-scaffolded Cu[I] PBA chain along with the triptycene-coordinated guest complex. (b) ORTEP of the T-shaped Cu1 complex. Ellipsoids for a and b are shown at the 50% probability level. (c) View of a single Cu[I] PBA chain. (d) View down the *a* axis showing the arrangement of the PBA chains. The Cu1 metal center has a T-shaped geometry with two N-coordinated cyanide ligands and one aqua ligand that is equally distributed between two orientations. The O1* coordination site on Cu1 is shown as partially transparent to denote a site occupancy of 0.5. (e) View down the *c* axis showing the stacking of the triptycene moieties and the isolated Cu[I] PBA chains. The aqua ligands on Cu1 have been omitted for clarity in this case.

consistent with a structure that is composed of weakly interacting metal complexes and also with the partially degraded PXRD pattern for the air-dried compound.

The orange plates **9** were first analyzed by IR spectroscopy to confirm formation of a PBA network and incorporation of **3** (see Supporting Information). The IR spectrum of **9** shows a broad cyanide stretching band at $\bar{\nu}_{CN} = 2110$ cm^{-1} that does not correspond to K$_3$[Fe(CN)$_6$] (narrow; $\bar{\nu}_{CN} = 2116$ cm^{-1}). Peaks attributable to the phenanthroline-extended triptycene are also observed in the IR spectrum. These data suggest incorporation of **3** into the metal cyanide network.

Single crystals of **9** suitable for X-ray diffraction were isolated from the product mixture. Figure 5 shows the solid-state structure of **9**. The first noticeable feature of the structure is the nature of the metal centers. Although K$_3$[Fe(CN)$_6$] was added to the reaction mixture, copper is the only metal present in the final structure. Under solvothermal conditions, K$_3$[Fe(CN)$_6$] becomes a source of cyanide but the Fe atoms were not incorporated into the PBA in this case. This behavior is well known for the Fe/Cu system, and a number of homometallic Cu[I] PBAs have been reported.[21,22,24,26,27] Three different geometries are observed for the Cu centers: T-shaped Cu1, pseudotrigonal planar

Cu2, and pseudotetrahedral Cu3 (Figure 5a and 5b). These geometries (all known for Cu[I] complexes), charge balance of the structure, and oxidation state of the precursor complex **8** strongly suggest that the Cu atoms in compound **9** are in the +1 oxidation state.

The structure of **9** is made of infinite one-dimensional zigzag Cu[I] cyanide chains extending in the direction of the *c* axis and separated by interdigitated triptycene ligands coordinated to the chains (Figure 5c and 5d). Strikingly, the voids between the triptycene pillars are filled with large intercalated guest complexes consisting of a tricoordinate Cu[I] center (Cu2) ligated by one triptycenyl phenanthroline and also one cyanide ligand. The chain itself is composed of cyanide-bridged pseudotetrahedral (Cu3) and T-shaped (Cu1) Cu[I] centers alternating in a Cu1—Cu3—Cu3—Cu1—Cu3—Cu3 fashion. The two Cu3 atoms next to each other in the chain are related by inversion symmetry, and as expected, the cyanide ligand bridging them (C66—N10) has no preferential orientation and is observed as disordered in the X-ray diffraction (hence the ligand having both C66 and N10 labels for each constituting atom in Figure 5). In addition to that disordered cyanide, the coordination sphere of Cu3 is composed of another C-bonded cyanide and a chelated ligand **3**. The Cu1 atom with T-shaped geometry has two pseudolinear N-bonded cyanide ligands and one aqua ligand (O1) (Figure 5b). Two partially occupied water sites coordinated to Cu1 were identified (site occupancy factor of 0.5). These data suggest that two equivalent orientations exist for O1. Regardless of its orientation, the aqua ligand on Cu1 is perfectly positioned to hydrogen bond with the nitrogen on the phenazine portion of **3** (N8 in Figure 5a). The O1* coordination site on Cu1 is shown as partially transparent in Figure 5c and 5d to highlight the site occupancy of 0.5 for the aqua ligand. It is worth noting that several chelated (bidentate or tridentate) T-shaped Cu[I] complexes have been reported recently.[40,41] In contrast, T-shaped Cu[I] complexes containing only monodentate ligands like the one observed in **9** are more unusual.[42]

Figure 5e shows the stacking of the triptycene moieties in the direction of the *c* axis and isolated Cu[I] PBA chains connecting the stacks along the *b* axis. The dppz moieties are separated by approximately 3.4 Å within the stacks, which is in the range for π stacking. The arrangement of the shape-persistent triptycenes results in void channels between the stacks running along the axis and these pores are filled with solvent molecules. Three molecules of methanol were located and modeled in the asymmetric unit (not shown in Figure 5).

At first glance, the dark brown cubic crystals of compound **10** appeared to be big enough for X-ray diffraction. Upon careful inspection, however, **10** turned out to be cubic particles of aggregated microcrystalline materials. As X-ray diffraction was unable to provide useful information about the identity of compound **10**, IR spectroscopy was employed to probe its nature. The IR spectrum of **10** shows a strong, broad band that can be assigned to the stretching mode of a cyanide species ($\bar{\nu}_{CN} = 2065$ cm^{-1}). The broadness of the peak is consistent with the cyanides in a bridging mode. No peaks corresponding to **3** (e.g., C—H stretching modes) are observed. These limited results suggest that **10** is the triptycene-free PBA byproduct left over from the solvothermal decomposition of K$_3$[Fe(CN)$_6$].

We attempted to use compounds **5** and **7** as scaffolding agents, employing the same solvothermal conditions as for **3**. Unfortunately, only amorphous or microcrystalline powders were obtained in all attempts and no further characterization was performed on

4556

dx.doi.org/10.1021/cg200788f |*Cryst. Growth Des.* 2011, 11, 4551–4558

these materials. The added phenanthroline units on compounds **5** and **7**, compared with **3**, and their increased bulk and internal molecular free volume presumably introduce additional restrictions for the building of a metal cyanide framework that in the end does not form under the conditions tested. In addition, poor solubility of the organic molecules in methanol, even at high temperature, might hinder formation of crystalline materials. Other solvents were also tested, but similar amorphous products were always isolated.

CONCLUSIONS

The molecular scaffolding of PBAs is an attractive goal as it could lead to materials with tunable and low-dimensional magnetic and electrochemical properties and with improved molecular storage capacities among others. In this work, we investigated the molecular scaffolding of a Cu^I cyanide PBA using phenanthroline-extended triptycene compounds as structure-directing ligands. The smallest member of this family, triptycenyl phenanthroline, forms a coordination complex with Cu^I ions when reacted with $CuCl_2$ in methanol under solvothermal conditions. It can be converted into a triptycene-scaffolded Cu^I PBA by heating it further in methanol under solvothermal conditions with $K_3[Fe(CN)_6]$, which acts as a source of cyanide. This homometallic PBA is composed of one-dimensional zigzag chains of cyanide-bridged Cu^I centers. The chains are separated by interdigitated phenanthroline-extended triptycene pillars, and the voids between the pillars are filled with large intercalated (triptycenyl phenanthroline) copper(I) cyanide guest complexes. Interestingly, three coordination geometries are observed for the Cu^I centers in the structure, including an unusual T-shaped complex with three monodentate ligands. The coordination chemistry developed here could not be generalized for the bigger phenanthroline-extended triptycene ligands such as triptycenyl bis(phenanthroline) and triptycenyl tris(phenanthroline).

Copper(I) cyanide coordination polymers based on *N*-heterocyclic ligands like the one described in this work are particularly interesting because of their strong fluorescence. Incorporation of porosity-generating triptycene derivatives into their structure and the structure of other PBAs could potentially allow small molecules to penetrate and interact with the bulk of the materials. We are continuing our pursuit of porous triptycene-containing frameworks.

ASSOCIATED CONTENT

ⓢ Supporting Information. Experimental details, crystallographic data, and additional characterization. This material is available free of charge via the Internet at http://pubs.acs.org.

AUTHOR INFORMATION

Corresponding Author
*E-mail: mmaclach@chem.ubc.ca.

ACKNOWLEDGMENT

REFERENCES

(1) Hoskins, B. F.; Robson, R. *J. Am. Chem. Soc.* **1989**, *111*, 5962–5964.

(2) Hoskins, B. F.; Robson, R. *J. Am. Chem. Soc.* **1990**, *112*, 1546–1554.

(3) Banerjee, R.; Phan, A.; Wang, B.; Knobler, C.; Furukawa, H.; O'Keeffe, M.; Yaghi, O. M. *Science* **2008**, *319*, 939–943.

(4) Yaghi, O. M.; O'Keeffe, M.; Ockwig, N. W.; Chae, H. K.; Eddaoudi, M.; Kim, J. *Nature* **2003**, *423*, 705–714.

(5) Kitagawa, S.; Kitaura, R.; Noro, S. *Angew. Chem., Int. Ed.* **2004**, *43*, 2334–2375.

(6) Latroche, M.; Surblé, S.; Serre, C.; Mellot-Draznieks, C.; Llewellyn, P. L.; Lee, J. H.; Chang, J. S.; Jhung, S. H.; Férey, G. *Angew. Chem., Int. Ed.* **2006**, *45*, 8227–8231.

(7) Lee, J.; Farha, O. K.; Roberts, J.; Scheidt, K. A.; Nguyen, S. T.; Hupp, J. T. *Chem. Soc. Rev.* **2009**, *38*, 1450–1459.

(8) Avendano, C.; Hilfiger, M. G.; Prosvirin, A.; Sanders, C.; Stepien, D.; Dunbar, K. R. *J. Am. Chem. Soc.* **2010**, *132*, 13123–13125.

(9) Korcok, J. L.; Katz, M. J.; Leznoff, D. B. *J. Am. Chem. Soc.* **2009**, *131*, 4866–4871.

(10) Sato, O.; Iyoda, T.; Fujishima, A.; Hashimoto, K. *Science* **1996**, *272*, 704–705.

(11) Ferlay, S.; Mallah, T.; Ouahès, R.; Veillet, P.; Verdaguer, M. *Nature* **1995**, *378*, 701–703.

(12) Shatruk, M.; Avendano, C.; Dunbar, K. R. In *Progress in Inorganic Chemistry*; John Wiley & Sons: New York, 2009; Vol. 56, pp 155−334.

(13) Kaye, S. S.; Long, J. R. *J. Am. Chem. Soc.* **2005**, *127*, 6506–6507.

(14) Bennett, M. V.; Shores, M. P.; Beauvais, L. G.; Long, J. R. *J. Am. Chem. Soc.* **2000**, *122*, 6664–6668.

(15) Ohkoshi, S.; Tokoro, H.; Hozumi, T.; Zhang, Y.; Hashimoto, K.; Mathonière, C.; Bord, I.; Rombaut, G.; Verelst, M.; Cartier dit Moulin, C. C.; Villain, F. *J. Am. Chem. Soc.* **2006**, *128*, 270–277.

(16) Beauvais, L. G.; Shores, M. P.; Long, J. R. *J. Am. Chem. Soc.* **2000**, *122*, 2763–2772.

(17) Zhang, J. J.; Lachgar, A. *J. Am. Chem. Soc.* **2007**, *129*, 250–251.

(18) Toma, L.; Lescouëzec, R.; Vaissermann, J.; Delgado, F. S.; Ruiz-Pérez, C.; Carrasco, R.; Cano, J.; Lloret, F.; Julve, M. *Chem.—Eur. J.* **2004**, *10*, 6130–6145.

(19) Lescouëzec, R.; Lloret, F.; Julve, M.; Vaissermann, J.; Verdaguer, M. *Inorg. Chem.* **2002**, *41*, 818–826.

(20) Gu, Z. Z.; Sato, O.; Iyoda, T.; Hashimoto, K.; Fujishima, A. *Chem. Mater.* **1997**, *9*, 1092–1097.

(21) Colacio, E.; Debdoubi, A.; Kivekäs, R.; Rodriguez, A. *Eur. J. Inorg. Chem.* **2005**, 2860–2868.

(22) Colacio, E.; Dominguez-Vera, J. M.; Lloret, F.; Sanchez, J. M. M.; Kivekas, R.; Rodriguez, A.; Sillanpaa, R. *Inorg. Chem.* **2003**, *42*, 4209–4214.

(23) Rodriguez, A.; Sakiyama, H.; Masciocchi, N.; Galli, S.; Galez, N.; Lloret, F.; Colacio, E. *Inorg. Chem.* **2005**, *44*, 8399–8406.

(24) He, X.; Lu, C. Z.; Yuan, D. Q.; Chen, S. M.; Chen, J. T. *Eur. J. Inorg. Chem.* **2005**, 2181–2188.

(25) Li, X. M.; Wang, C. F.; Ji, Y.; Kang, L. C.; Zhou, X. H.; Zuo, J. L.; You, X. Z. *Inorg. Chem.* **2009**, *48*, 9166–9173.

(26) Liang, S. W.; He, X.; Shao, M.; Li, M. X. *J. Coord. Chem.* **2008**, *61*, 2999–3007.

(27) Mao, H. Y.; Zhang, C. Z.; Xu, C.; Zhang, H. Y.; Shen, X. Q.; Wu, B. L.; Zhu, Y.; Wu, Q. G.; Wang, H. *Inorg. Chim. Acta* **2005**, *358*, 1934–1942.

(28) Chong, J. H.; Ardakani, S. J.; Smith, K. J.; MacLachlan, M. J. *Chem.—Eur. J.* **2009**, *15*, 11824–11828.

(29) Chong, J. H.; MacLachlan, M. J. *Inorg. Chem.* **2006**, *45*, 1442–1444.

(30) Chong, J. H.; MacLachlan, M. J. *J. Org. Chem.* **2007**, *72*, 8683–8690.

(31) Chong, J. H.; MacLachlan, M. J. *Chem. Soc. Rev.* **2009**, *38*, 3301–3315.

(32) Ghanem, B. S.; Hashem, M.; Harris, K. D. M.; Msayib, K. J.; Xu, M. C.; Budd, P. M.; Chaukura, N.; Book, D.; Tedds, S.; Walton, A.; McKeown, N. B. *Macromolecules* **2010**, *43*, 5287–5294.

(33) Ghanem, B. S.; Msayib, K. J.; McKeown, N. B.; Harris, K. D. M.; Pan, Z.; Budd, P. M.; Butler, A.; Selbie, J.; Book, D.; Walton, A. *Chem. Commun.* **2007**, 67–69.

(34) Long, T. M.; Swager, T. M. *J. Am. Chem. Soc.* **2003**, *125*, 14113–14119.

(35) Munakata, M.; Wu, L. P.; Sugimoto, K.; Kuroda-Sowa, T.; Maekawa, M.; Suenaga, Y.; Maeno, N.; Fujita, M. *Inorg. Chem.* **1999**, *38*, 5674–5680.

(36) Vagin, S.; Ott, A.; Weiss, H. C.; Karbach, A.; Volkmer, D.; Rieger, B. *Eur. J. Inorg. Chem.* **2008**, 2601–2609.

(37) Jiang, Y.; Chen, C. F. *Synlett* **2010**, 1679–1681.

(38) Amouyal, E.; Homsi, A.; Chambron, J.-C.; Sauvage, J.-P. *J. Chem. Soc., Dalton Trans.* **1990**, 1841–1845.

(39) Healy, P. C.; McMurtrie, J. C.; Bouzaid, J. *Acta Crystallogr., Sect. E.: Struct. Rep. Online* **2010**, *66*, M493–U271.

(40) van der Vlugt, J. I.; Pidko, E. A.; Vogt, D.; Lutz, M.; Spek, A. L. *Inorg. Chem.* **2009**, *48*, 7513–7515.

(41) Hu, X.; Castro-Rodriguez, I.; Meyer, K. *J. Am. Chem. Soc.* **2003**, *125*, 12237–12245.

(42) Zheng, L.-M.; Yin, P.; Xin, X.-Q. *Inorg. Chem.* **2002**, *41*, 4084–4086.